1998

Ballistic Transport in Ultrathin Films with Random Rough Walls

A. E. Meyerovich
University of Rhode Island, sfo101@uri.edu

S. Stepaniants

Citation/Publisher Attribution
A.E. Meyerovich, S.Stepaniants. Ballistic Transport in Ultrathin Films with Random Rough Walls *J.Phys.:Condens.Matter.,* 9, 4157 (1997).
Available at: http://dx.doi.org/10.1088/0953-8984/9/20/015

Ballistic transport in ultrathin films with random rough walls

A.E.Meyerovich † and S.Stepaniants ‡

Department of Physics, University of Rhode Island, Kingston, RI 02881, USA

Abstract. We calculated transport coefficients in thin films in which the particle wavelength is comparable to the thickness of the film, and the motion across the film is quantized. The perturbative calculations are analytical almost to the very end, and result in explicit transparent expressions for the transport coefficients via the correlation function of surface inhomogeneities, density of particles, and film thickness. The final results are given for Gaussian correlations of the surface inhomogeneities. The discrete nature of the spectrum leads to a non-analyticity of transport coefficients as a function of particle density and film thickness, especially for degenerate fermions. Surface inhomogeneity causes both in-band scattering and interband transitions; the role of interband transitions is determined by the correlation radius of surface inhomogeneities. The shape of the curves for the dependence of transport coefficients on the number of particles and film thickness is determined by the correlation of surface inhomogeneities and is not very sensitive to their amplitude. For short range correlations, the interband transitions lead to a saw-like shape of the curves. With an increasing correlation radius, the interband transitions become suppressed, and the saw teeth gradually decrease, reducing, in the end, to small kinks on otherwise monotonic curves. Careful analysis of the transition from quantum to semiclassical and classical regimes allowed us to improve the accuracy of our previous classical calculations.

Short title: Ballistic transport in ultrathin films with random rough walls

August 21, 1998

† To whom correspondence should be addressed

‡ Present address: Beckman Institute, University of Illinois, 405 N.Mathews Ave., Urbana, IL 61801, USA

1. Introduction

Repeated collisions of ballistic particles with rough walls with random inhomogeneities restrict particle motion along the walls, and are responsible for the formation of the mean free path, quantum interference effects, and localization. Scattering of particles and waves by random rough walls is an old and thoroughly studied problem (see books [1, 2, 3, 4, 5, 6, 7]). However, most of the existing *transport* calculations for the wall-imposed limitations on the transport coefficients and mean free path along the walls, involve either oversimplified models or complicated integro-differential boundary conditions (see, *e.g.,* reviews [8, 9] and references therein). The lack of simple expressions for the transport coefficients via statistical characteristics of surface inhomogeneities hinders experimental and theoretical work on systems with long free paths.

Recently we suggested a simple perturbative description of ballistic transport in systems with random rough walls [10] (see also [11]). We expressed transport and localization parameters such as mobility, diffusion, mean free path, localization length, *etc.,* for *ballistic* particles directly via the wall profile, namely, via the correlation function of wall inhomogeneities. Despite an intensive previous work on transport in thin films and channels with rough walls and a large amount of available data, our transparent semi-analytical results provide a new explicit link between the transport coefficients and the correlation function of surface inhomogeneities (for the latest experimental and theoretical results on transport see Refs.[10, 12, 13, 14, 15] and references therein).

Our calculations were based on a canonical coordinate transformation, similar to the Migdal transformation in nuclear physics, which makes the rough boundaries flat, but complicates the bulk equations. This idea was proposed earlier in Refs.[16, 17], but was not carried out explicitly. We used an explicit expression for the coordinate transformation with the parameters given by the exact profile of the random boundaries. This provides an exact reformulation of the transport problem with random rough walls as the transport problem with flat walls and randomly distorted bulk. The arising bulk problem can be solved using the standard semiclassical perturbative transport equation.

The idea to reduce a surface scattering problem to a bulk one has been used successfully in other fields, including the electromagnetic and acoustic wave scattering, diffraction patterns, wave guides, *etc.*, for several decades (see, *e.g.*, [2, 6, 18, 19, 20, 21, 22, 23, 24, 25] and references therein). Generally speaking, such a reduction, either in the form of direct coordinate transformation or as an expansion in initial boundary conditions, is inherent to perturbative calculations for small roughness.

Our procedure is the first explicit application of such a technique developed specifically for ballistic transport in thin films and narrow channels. The calculations are analytical almost to the very end. The transparent results express transport coefficients directly via the correlation functions of surface inhomogeneities, and can be used for

analysis of experimental data or as a basis for further calculations. Apart from the transport coefficients, such as mobility and diffusion in different physical systems, the method provides a simple tool for the study of wall-induced localization and quantum interference effects thus supplementing the localization results of Refs.[21, 25, 26, 27, 14]. Since we are interested in slight roughness, the calculation of the "classical" mean free path should precede and serve as a basis for the calculation of the (small) quantum interference effects and (weak) localization with (exponentially) large localization length. [In the case of strong roughness, the *transport* problem is simple: the mean free path becomes equal to the film thickness with the obvious consequences for transport coefficients. Other problems for strong roughness, such as quantum interference effects or wave patterns for wave scattering, remain non-trivial].

In this paper we study ballistic transport in very thin films with quantized motion of particles across the film, $p_x \sim j\hbar/L$ (L is the average distance between the walls, j is the quantum number). The quantization is important for electron transport in ultra-thin pure metal films and for microflows and microdevices (see Ref.[28] and references therein). In thin films with discrete levels for motion across the film, the change in particle density N and/or film thickness L causes the redistribution of particles between these levels. In Fermi systems at $T \to 0$ this is a non-analytical step-like process which should lead to singularities in the dependence of the transport coefficients on the density of particles or film thickness. The density dependence of the transport coefficients should become more and more smooth with increasing temperature even for a distinctly discrete energy spectrum.

Similar singularities in transport in ultra-thin films have already been described for scattering on bulk impurities [29], and have been qualitatively suggested in Ref.[17] for scattering by rough walls. [Note, that this saw-like effect is a purely "classical" transport result that has nothing in common with $1D$ quantization of conductance for an effectively $1D$ motion of particles through a narrow contact[14, 27]]. Recent perturbative approach to a similar problem [15] included bulk attenuation, but disregarded the role of the correlation radius R and missed the operator $\hat{x}\hat{p}_x$ in the perturbation (this operator is inherent to such problems [16] and is responsible for interlevel transitions). As we will see, the value of the correlation radius R and the interlevel transitions define the shape of the dependence of transport coefficients on film thickness and/or particle density.

In the next Section we present general perturbative equations for quantized transport in thin films with rough boundaries. In Sec.3 we study transport singularities for degenerate fermions at $T = 0$. In Sec.4 we analyze transport at finite temperature, and calculate the transport coefficients in the Boltzmann temperature range. The results ensure a consistent transition from discrete to continuous expressions, and improve the accuracy of our previous calculations [10] for continuous spectrum in the classical and semi-classical limits. The improved results for classical transport are given in the

Appendix. The final results are presented for the Gaussian correlation of the surface inhomogeneities; similar calculations can also be done for other types of correlation functions.

2. Transport of particles with quantized motion across the channels

We will consider a film (channel) of the average thickness L with rough boundaries $x = L/2 - \xi_1(y,z)$ and $x = -L/2 + \xi_2(y,z)$. The small boundary inhomogeneities, $\xi_1(y,z), \xi_2(y,z) \ll L$, are random functions of coordinates $\mathbf{s} = (y,z)$ along the boundaries, $\langle \xi_1 \rangle = \langle \xi_2 \rangle = 0$. The correlation function $\langle \xi_i(\mathbf{s}_1)\xi_k(\mathbf{s}_2)\rangle$ depends only on the distance between points $|\mathbf{s}_1 - \mathbf{s}_2|$ and not on coordinates themselves,

$$\zeta_{ik}(|\mathbf{s}_1 - \mathbf{s}_2|) = \langle \xi_i(\mathbf{s}_1)\xi_k(\mathbf{s}_2)\rangle, \quad \zeta_{ik}(\mathbf{q}) = \int d^2 s \; e^{i\mathbf{q}\cdot\mathbf{s}/\hbar}\zeta_{ik}(\mathbf{s}). \tag{1}$$

Our approach is based on the canonical coordinate transformation $\mathbf{r} \to \mathbf{R}$, $\mathbf{p} \to \mathbf{P}$,

$$X = \frac{L[x - (\xi_2(y,z) - \xi_1(y,z))/2]}{L - (\xi_1(y,z) + \xi_2(y,z))}, \; Y = y, \; Z = z \tag{2}$$

which makes the walls flat, $X = \pm L/2$, and is responsible for the following change in the form of the bulk Hamiltonian $\widehat{H} = p^2/2m$:

$$\widehat{H} = \frac{\widehat{P}^2}{2m} + \widehat{V}_x + \widehat{V}_y + \widehat{V}_z, \; \widehat{V}_x = \frac{\xi}{mL}\widehat{P}_x^2, \tag{3}$$

$$\widehat{V}_y = \frac{X}{2mL}\left[\xi_y'\widehat{P}_x\widehat{P}_y + \widehat{P}_x\xi_y'\widehat{P}_z\right] - \frac{1}{4m}\left[\left(\xi_{2y}' - \xi_{1y}'\right)\widehat{P}_x\widehat{P}_y + \widehat{P}_x\left(\xi_{2y}' - \xi_{1y}'\right)\widehat{P}_z\right]$$

where $\xi = \xi_1 + \xi_2$ and $\widehat{V}_z$ is similar to $\widehat{V}_y$; see [10] for details. The randomness of inhomogeneities, $\langle \xi_{1,2} \rangle = 0$, leads to the randomness of the bulk distortion $\widehat{V}$, $\left\langle \widehat{V} \right\rangle = 0$. Thus, the transformation (2) reduces the transport problem between rough walls to an equivalent transport problem with ideal specular walls, $\Psi(L/2) = \Psi(-L/2) = 0$ and distorted bulk Hamiltonian (3). The latter problem can be treated in the same standard perturbative way as any random bulk imperfections or impurities.

The perturbative approach to surface roughness requires that the surface inhomogeneities should be relatively smooth with the amplitude ℓ smaller than their correlation radius R and the thickness of the film L, $\ell \ll L, R$. The use of a semiclassical transport equation for the motion along the film imposes an additional condition on the wavelength, namely, that the wall-induced distorting force does not change the energy along the wall on the scale $1/q$ (q is the characteristic wave vector for particle motion along the walls). In the case of not very high quantum numbers j for the motion across the film, this means that either $\ell/L \ll q^2R^2$, q^3RL^2 or $1 \ll qR$; if both inequalities are broken, one should substitute the Poisson bracket in the transport equation by the exact quantum commutator. These conditions have different meanings for thin films

with microscopic roughness, $R \ll L$, and for smooth films that are irregularly curved on a macroscopic scale, $R \gg L$. When, as it is often the case, the wave vector along the film q is of the same order as for the motion across the film, $q \sim 1/L$, the applicability of our perturbative semiclassical approach requires $\ell \ll L,\ R,\ R^2/L$.

The effective bulk distortion (3) determines the effect of surface roughness on transport via the Born collision integral

$$L_j = \frac{2\pi}{\hbar} \sum_{j'} \int \left\langle \left| V_{\mathbf{jq},j'\mathbf{q}'} \right|^2 \right\rangle \left[n_j(1-n'_{j'}) - n'_{j'}(1-n_j) \right] \times \qquad (4)$$
$$\delta\left(\epsilon_j(\mathbf{q}) - \epsilon'_{j'}(\mathbf{q}') \right) \frac{d^2q'}{(2\pi\hbar)^2}$$

in the transport equation for the subbands j

$$\partial_t n(\epsilon_j, \mathbf{q}) + \frac{\mathbf{q}}{m} \cdot \partial_{\mathbf{r}} n(\epsilon_j, \mathbf{q}) + \mathbf{F} \cdot \partial_{\mathbf{q}} n(\epsilon_j, \mathbf{q}) = L_j\{n_i\} \qquad (5)$$

where subbands $\epsilon_j(\mathbf{q}) = \left[(\pi j\hbar/L)^2 + q^2 \right]/2m$. The equation includes both in-band scattering and interband transitions. Since we are interested in the effects of slight roughness in the lowest approximation, we do not have to include the roughness-induced corrections to the energy levels, and can neglect all the roughness corrections to the *l.h.s.* of Eq.(5). The collision integral (4) and , therefore, the transport coefficients contain the squares of the matrix elements of the "perturbation" $\widehat{V}$, and the averaging over the random surface inhomogeneities leads directly to the correlation function $\zeta(\mathbf{s})$.

The calculation of the matrix elements $\left\langle \left| V_{\mathbf{jq},j'\mathbf{q}'} \right|^2 \right\rangle$ with the unperturbed wave functions $\Psi_j = \sqrt{2/v_0} \exp(i\mathbf{q}\cdot\mathbf{s}) \sin(\pi j X/L)$ is trivial (v_0 is the volume). The Hamiltonian (3) contains terms with $\xi = \xi_1 + \xi_2$ and $\xi_1 - \xi_2$. Both terms contribute to the matrix elements $\left| V_{\mathbf{jq},j'\mathbf{q}'} \right|^2$ and the collision integral (4). After the averaging and integration with the δ-functions in (4), the term with $\xi_1 - \xi_2$ becomes equal to zero, as in [10]. This cancellation occurs only because of the randomness of surface roughness *and* the absence of bulk collisions. In the case of regular roughness (*i.e.,* periodic walls or channels of finite length) or in the presence of particle-particle and particle-impurity bulk collisions the contribution of $\xi_1 - \xi_2$ is finite. In our case of ballistic transport between random-rough walls, the terms with $\xi_1 - \xi_2$ disappear from the collision integral (4):

$$L_j = \frac{1}{2\pi\hbar^3 m^2 L^2} \int d^2q'\, \zeta(\mathbf{q}-\mathbf{q}') \sum_{j'} \left(n_{j'}(\mathbf{q}') - n_j(\mathbf{q}) \right) \delta\left(\epsilon_{j'\mathbf{q}'} - \epsilon_{j\mathbf{q}} \right) \times$$
$$\left[\delta_{jj'} \left(\frac{1}{4}(\mathbf{q}-\mathbf{q}')^2 + \left(\frac{\pi\hbar j}{L} \right)^2 \right)^2 + \frac{(1-\delta_{jj'})\, j^2 j'^2}{\left(j^2 - j'^2\right)^2} \left(q'^2 - q^2 \right)^2 \right]. \qquad (6)$$

where $\zeta(\mathbf{q}) = \zeta_{11} + \zeta_{22} + 2\zeta_{12}$ is the Fourier component of the correlation function $\langle \xi(\mathbf{s}_1)\, \xi(\mathbf{s}_2) \rangle$ for $\xi = \xi_1 + \xi_2$ (see Eq.(1)).

The transport equation (5) , (6)is a set of equations in the distribution functions n_j coupled via collision integrals L_j. We can solve the transport equation for an arbitrary correlation function $\zeta(\mathbf{q})$ and express the transport coefficients via the zeroth and first angular harmonics of the correlation function at different values of q. We will supplement the general expressions by the most practical example of the Gaussian correlations of the surface inhomogeneities of an average height ℓ,

$$\zeta(\mathbf{s}) = \ell^2 \exp\left(-s^2/2R^2\right), \quad \zeta(\mathbf{q}) = 2\pi\ell^2 R^2 \exp\left(-q^2R^2/2\hbar^2\right) \tag{7}$$

including the δ-type correlations in the limit of the small correlation radius R,

$$\zeta(\mathbf{s}) = \ell^2 R^2 \delta(s)/s, \quad \zeta(\mathbf{q}) = 2\pi\ell^2 R^2 \tag{8}$$

The condition $\ell \ll R$ does not mean that our approach is applicable only to the long-range correlations (large size inhomogeneities). The scale for the effective correlation range in Eq.(7) is defined by the particles wavelength $\lambda \sim 1/q$. If $\lambda \gg R$, one deals with the short-range δ-type correlations (8), while in the opposite case of long-range correlations $\lambda \ll R$ one should consider the full Gaussian expression (7). Only the large number of equations (5) (relevant subbands j) prevents us from giving a fully analytical solution of the transport problem.

3. Singularities in transport of particles with discrete quantum states: Low temperatures

Changes in particle density and/or thickness of the film lead to the redistribution of particles between subbands with different j. This redistribution between *discrete* states may lead to a non-analytic dependence of transport coefficients on particle density and thickness of the film [17]. This non-analyticity is more pronounced for degenerate Fermi systems at $T \to 0$ when continuous increase in the number of particles leads, at certain critical densities, to filling of new levels with higher and higher values of j.

At $T = 0$, the Fermi momenta of fermions for the motion along the film $q_F^{(j)}$in each subband j are given by the overall Fermi energy ϵ_F as

$$\epsilon_F = \frac{1}{2m}\left(\left(\frac{\pi j\hbar}{L}\right)^2 + q_F^{(j)2}\right) \tag{9}$$

while the $2D$ density of spin-1/2 particles in subbands

$$N_j = \frac{q_F^{(j)2}}{2\pi\hbar^2} \tag{10}$$

(for simplicity we assume that the effective masses of particles in all subbands are the same). The chemical potential $\mu = \epsilon_F$ is determined self-consistently by calculating the

total density of particles N,

$$N = \sum_j N_j = \frac{1}{2\pi\hbar^2} \sum_j \left(2m\epsilon_F - \left(\frac{\pi j \hbar}{L} \right)^2 \right). \tag{11}$$

Eqs. (9)-(11) in convenient dimensionless notations,

$$\nu = 2m\epsilon_F \left(\frac{L}{\pi\hbar} \right)^2, \; z_j = \frac{2}{\pi} N_j L^2, \; z \equiv \sum_j z_j = \frac{2}{\pi} N L^2, \tag{12}$$

can be rewritten as

$$z_j = \nu - j^2, \; z = \sum z_j \tag{13}$$

The number of occupied levels S for the given value of z (*i.e.*, for the number of particles NL^2) is given by the integer part of $\nu^{1/2}(z)$,

$$S(z) = \text{Int} \left[\sqrt{\nu} \right] \tag{14}$$

All the levels with the indices $j > S$ are empty, $z_{j>S} = 0$. Summation in Eqs.(13) from 1 to S defines the number of occupied levels S and the dimensionless chemical potential ν as functions of the number of particles z:

$$\begin{aligned} S \quad &= \text{Int} \left[\sqrt{\nu} \right] = \text{Int} \left[\sqrt{\frac{z}{S} + \frac{(S+1)(2S+1)}{6}} \right], \\ \nu(z) \; &= \frac{z}{S} + \frac{1}{6}(S+1)(2S+1) \end{aligned} \tag{15}$$

[For computational purposes, it is convenient to start from defining the number of occupied levels S, and to determine the interval of the values of z and ν, which corresponds to this number of levels, basing on the value of S]. The changes in number of occupied levels $S = 1,\ 2,\ 3,\ 4,\ 5,\ 6, \ldots$ occur at $z = 0,\ 3,\ 13,\ 34,\ 70,\ 125, \ldots$ (*i.e.*, in the points $z = S^3 - S(S+1)(2S+1)/6$).

At $T = 0$, we look for the solution of the transport equation (5) in the form

$$n_j(\mathbf{q}) = n_j^{(0)} \left(q_F^{(j)} \right) - \frac{FL^3}{\pi^4 \ell^2} \delta(\epsilon - \epsilon_F) \chi_j \left(q_F^{(j)} \right) \cos\theta_j,$$

where θ_j is the angle between the momentum $\mathbf{q}_j$ and the external force $\mathbf{F}$. Then, after the integration of the collision integral (6) with the Gaussian correlation of surface inhomogeneities (7), the transport equation reduces to the following set of S dimensionless linear equations in $\chi_j \left(q_F^{(j)} \right)$ with hypergeometric coefficients:

$$\begin{aligned} \frac{z_j^{1/2} L^2}{R^2} = -\frac{1}{2}\chi_j \Bigg(& 4j^4 \, {}_1F_1 \left(\tfrac{3}{2}, 2, -\tfrac{2\pi^2 z_j R^2}{L^2} \right) + 6 z_j j^2 \, {}_1F_1 \left(\tfrac{5}{2}, 3, -\tfrac{2\pi^2 z_j R^2}{L^2} \right) \\ & + \tfrac{5}{2} z_j^2 \, {}_1F_1 \left(\tfrac{7}{2}, 4, -\tfrac{2\pi^2 z_j R^2}{L^2} \right) \Bigg) \\ & + 2 \sum_{j'}^{S(z)} (1 - \delta_{jj'}) \, j^2 j'^2 \exp \left[-\pi^2 \left(\sqrt{z_j} - \sqrt{z_{j'}} \right)^2 R^2 / 2L^2 \right] \times \end{aligned} \tag{16}$$

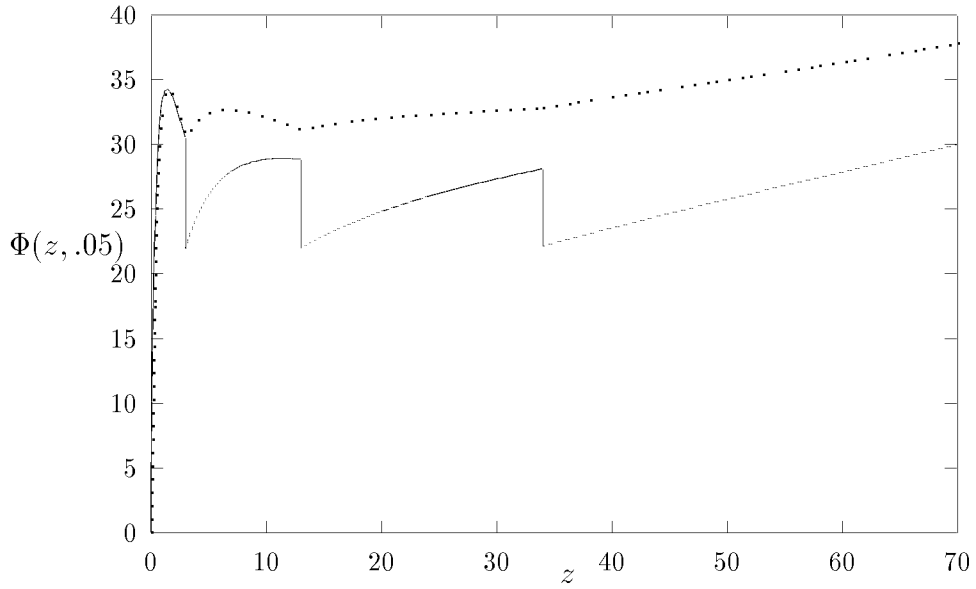

Figure 1. $\Phi(z, R/L)$, Eq.(18), as a function of density $z = 2NL^2/\pi$ for the correlation radius $R/L = 0.05$. Solid line - exact calculation; dotted line - calculation without interband transitions (without off-diagonal terms in the collision integral Eq.(6))

$$\left[\begin{array}{c} \chi_{j'}\left({}_1F_1\left(\frac{1}{2},1,-\frac{2\pi^2\sqrt{z_j z_{j'}}R^2}{L^2}\right)-{}_1F_1\left(\frac{3}{2},2,-\frac{2\pi^2\sqrt{z_j z_{j'}}R^2}{L^2}\right)\right) \\ -\chi_j\,{}_1F_1\left(\frac{1}{2},1,-\frac{2\pi^2\sqrt{z_j z_{j'}}R^2}{L^2}\right) \end{array}\right]$$

[We do not give cumbersome equations for the correlation function of a general form $\zeta(\mathbf{q})$ with the coefficients expressed via the angular harmonics of the correlation function on the Fermi surface]. The conductivity (mobility) of particles is given by the solution of this set of equations as

$$\sigma_{yy} = \sigma_{zz} = \sum_{j=1}^{S} \sigma_{yy}^{(j)} = -\frac{e^2L^2}{2\pi^4\hbar\ell^2} \sum_{j=1}^{S} z_j^{1/2} \chi_j\left(q_F^{(j)}\right), \tag{17}$$

and can be conveniently parametrized in the form

$$\sigma_{yy} = \sigma_{zz} = \frac{e^2L^2}{\pi^4\hbar\ell^2}\Phi\left(z, \frac{R}{L}\right), \quad z = \frac{2}{\pi}NL^2 \tag{18}$$

The dimensionless functions $\Phi(z, R/L)$ for four different values of R/L are plotted in Figure 1 (solid line) for $R/L = 0.05$, and in Figure 2 for $R/L = 1; 3; 5$. The singular points correspond to change in values of S from 1 to 2 to 3 to 4... at $z = 3;\ 13;\ 34;...$

This representation gives the dependence of the conductivity (mobility) on the dimensionless density of particles NL^2 for different (dimensionless) correlation radii R/L. Another possible way of parameterization of the equations, similar to the one

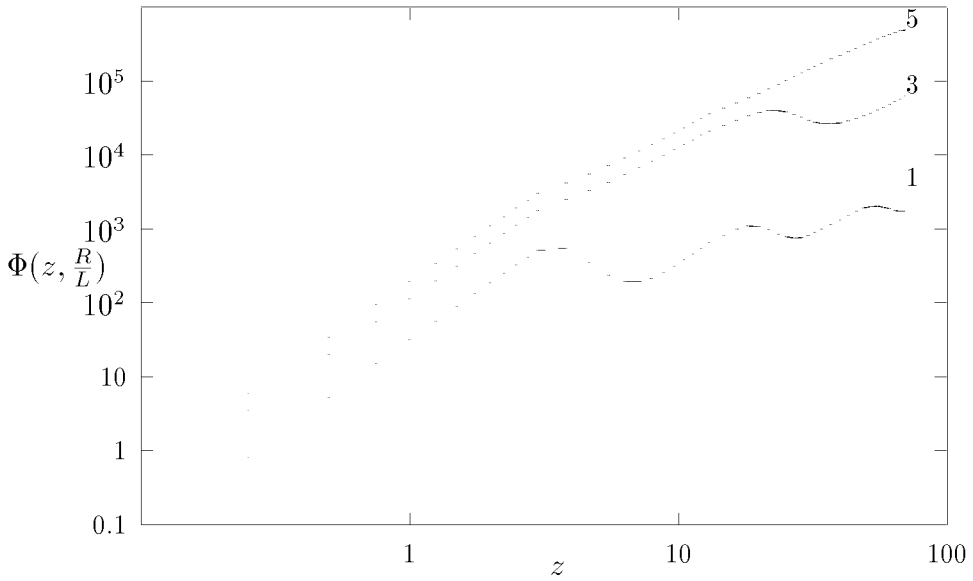

Figure 2. $\Phi(z, R/L)$, Eq.(18), as a function of density $z = 2NL^2/\pi$ for the correlation radius $R/L = 1; 3; 5$. The curves are labeled by the values of R/L

used in [10], could be based on the definition

$$\frac{2\pi^2\sqrt{z_j z_{j'}}R^2}{L^2} = \frac{4\pi\sqrt{z_j z_{j'}}NR^2}{z} = \frac{8\pi^2\sqrt{z_j z_{j'}}}{z}\left(\frac{R}{\lambda}\right)^2,$$

where the effective particle wavelength $\lambda^2 = 2\pi/N$. This equation redefines the function $\Phi(z, L/R)$ in (18) as $\Phi^{(1)}(z, R/\lambda) = \Phi(z, 2R/\lambda\sqrt{z})$ or as $\Phi^{(2)}\left(z, R\sqrt{N}\right) = \Phi\left(z, \sqrt{2N/\pi z}R\right)$. These alternative parametrizations would give the conductivity (mobility) as a function of dimensionless thickness $L\sqrt{N}$ at different correlation radii $R\sqrt{N}$ or R/λ. The z-dependences of the conductivity for all these parametrizations look roughly the same.

The diffusion coefficient $D_{yy} = D_{zz}$ is related to the mobility (21) as

$$D_{yy} = -\frac{\pi\hbar^2}{e^2 m}\sigma_{yy}/\sum_{j=1}^{S}\int\frac{\partial n_j}{\partial\epsilon}d\epsilon = \frac{\pi\hbar^2\sigma_{yy}}{e^2 mS} = \frac{L^2\hbar}{\pi^3 m\ell^2 S}\Phi\left(z, \frac{R}{L}\right), \tag{19}$$

while the mean free path along the channel is

$$\mathcal{L} = \frac{\sigma < q >}{e^2 N} = \frac{(2\pi)^{1/2}\hbar\sigma}{e^2 N^{3/2}}\left(\sum N_j^2\right)^{1/2} \sim L\frac{LR}{\ell^2}\frac{L}{R}\frac{\Phi(z, R/L)}{z} \tag{20}$$

Dramatic difference in shapes of the curves in Figures 1 and 2 for small and large values of R/L is explained by the role of interlevel transitions. If one neglects the interband transitions (the off-diagonal matrix elements $\widehat{V}_{jj'}$ with $j' \neq j$) in the collision integral (6), then the set of transport equations (16) will decouple into S independent

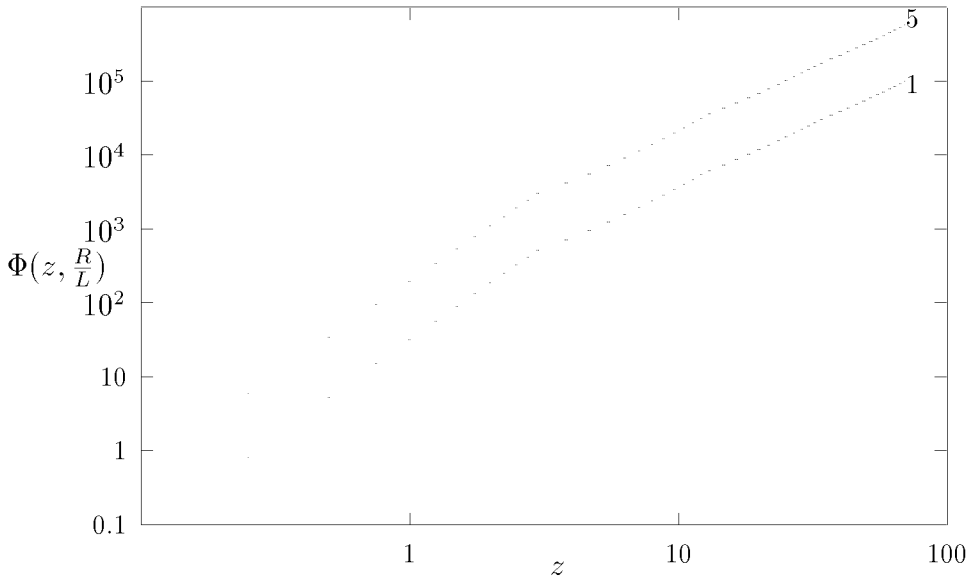

Figure 3. $\Phi(z, R/L)$, Eq.(18), as a function of z for $R/L = 1; 5$ caculated without interlevel transitions (without off-diagonal terms in the collision integral (6). The curves are labled by the values of R/L

equations. It is obvious that in this approximation the conductivity should be an almost monotonic function of $z = 2NL^2/\pi$, though the critical values of z, which correspond to the change in the number of occupied levels S, are still responsible for the singularities (small kinks) in the curves. Therefore, the saw-like nature of the curves is caused by the interlevel transitions exclusively.

For comparison, Figure 1 (dashed line) and Figure 3 give the function $\Phi(z)$ calculated when all the interband off-diagonal terms $j' \neq j$ in the collision integral (6) are artificially disregarded. The curves with and without transitions always coincide as far as $z \leq 3$ when there is only one occupied subband. The differences show up only at $z > 3$.

Algebraically, the importance of interband transitions is characterized by the parameter $NR^2 \sim zR^2/L^2$. Since $z_{j'} - z_j = j^2 - j'^2$, the exponents in Eqs.(16)

$$\exp\left[-\pi^2\left(\sqrt{z_j} - \sqrt{z_{j'}}\right)^2 R^2/2L^2\right] \equiv \exp\left[-\pi\left(\sqrt{N_j R^2} - \sqrt{N_{j'} R^2}\right)^2\right]$$

make interlevel transitions to remote levels $|j - j'| \gg L/R$ negligible. These exponents show also that the interband transitions and the resulting mixing of adjacent levels are very important only for not very populated levels with $2\pi^2 z_j R^2/L^2 \ll 1$. Thus, the contribution of interband transitions is noticeable only for relatively small values of R/L, and decreases exponentially with increasing R/L. For this reason, the saw-like character of particles mobility becomes less and less pronounced with increasing R/L.

At $R/L = 5$ the saw nearly completely disappears, and there is practically no difference between the curves in Figure 2 (exact calculation) and Figure 3 (calculation without interband transitions). Note, that the curves calculated with and without transitions always coincide for a small number of particles $z < 3$ when only one level is occupied and the transitions are impossible for energy reasons.

The same parameters, $2\pi^2 z_j R^2/L^2 = 4\pi N_j R^2$, determine the values of the hypergeometric functions in (16). At $x^2 \ll 1$, ${}_1F_1\left((2n-1)/2, n, -x^2\right) \simeq 1$, while in the opposite case $x^2 \gg 1$, ${}_1F_1\left((2n-1)/2, n, -x^2\right) \simeq (n-1)!/\sqrt{\pi}x^n$. Therefore, at large $2\pi^2 z_j R^2/L^2 \gg 1$, one can not only neglect the interband transitions, but also the hypergeometric functions ${}_1F_1\left((2n-1)/2, n, -x^2\right)$ with $n = 3$ and $n = 4$ in the diagonal terms of the collision integrals (16) in comparison with the one with $n = 2$. Under these conditions one can justify a heuristic assumption made in [10] and recover the result (53):

$$\sigma_{yy} = \sum_{j=1}^{S} \sigma_{yy}^{(j)} = \frac{e^2 L^2}{\pi^4 \hbar \ell^2} \Phi\left(z, \frac{R}{L}\right), \tag{21}$$

$$\Phi\left(z, \frac{R}{L}\right) = \frac{L^2}{4R^2} \sum_{1}^{S(z)} \frac{1}{j^4} \frac{z_j}{{}_1F_1\left(\frac{3}{2}, 2, -2\pi^2 z_j R^2/L^2\right)}.$$

If the correlation radius is small, $NR^2 \ll 1$, all the terms in (16) are of the same order, while the hypergeometric function ${}_1F_1\left((2n-1)/2, n, -2\pi^2 z_j R^2/L^2\right) \sim {}_1F_1\left((2n-1)/2, n, 0\right) = 1$. Then Eqs.(16) can be simplified as

$$\frac{z_j^{1/2} L^2}{R^2} = -\frac{1}{2}\chi_j \left(4j^4 + 6z_j j^2 + \frac{5}{2} z_j^2\right) - 2\chi_j \sum_{j'}^{S(z)} \left(1 - \delta_{jj'}\right) j^2 j'^2 \tag{22}$$

In this case

$$\Phi\left(z, \frac{R}{L}\right) = \frac{L^2}{4R^2} \sum_{j=1}^{S(z)} \frac{\nu(z) - j^2}{\left(j^4 + 3z_j j^2/2 + 5z_j^2/8\right) + S(S+1)(2S+1)/6 - j^2} \tag{23}$$

In the opposite limit when $z_j R^2/L^2 \gg 1$ for all j, the interlevel transitions and higher-order hypergeometric functions can be neglected, ${}_1F_1\left(\frac{3}{2}, 2, -x^2\right) \to 1/\sqrt{\pi}x^3$, and

$$\Phi\left(z, \frac{R}{L}\right) = \frac{\pi^{7/2} R}{2^{1/2} L} \sum_{j=1}^{S(z)} \frac{\left(\nu(z) - j^2\right)^{5/2}}{j^4} \tag{24}$$

Note that the accuracy of Eq.(24) for large NR^2 can be improved near the critical values of z which correspond to changes in number of occupied levels S. With the appearance of a new level S, the number of particles on this level, z_S, and, therefore, $z_S R^2/L^2$ are small even for large R/L, and the contribution of this level is $z_S/\,{}_1F_1\left(\frac{3}{2}, 2, -2\pi^2 z_s R^2/L^2\right) \sim z_S$, and not $z_S \pi^{1/2} \left(2\pi^2 z_S R^2/L^2\right)^{3/2}$ as it is implied by

Eq.(24). Away from the critical density the hypergeometric function becomes small, $2\pi^2 z_S R^2/L^2 \gg 1$, and the contribution of this highest level will recover the form indicated by (24).

The argument of the exponents and hypergeometric functions can be also written as the ratio of the particle wavelength to the correlation radius of surface inhomogeneities, $2\pi^2 z_j R^2/L^2 \sim (R/\lambda_j)^2$. The particle wavelength serves as a natural scale for describing the correlations and separates long-range from short-range correlations. In this sense, the interband transitions are more important for the short-range correlations.

4. Transport along films and channels: High temperatures

At finite temperatures, all the levels with different j are populated, and the transport equation is an infinite set of coupled equations (5). The chemical potential is the same for particles in all bands,

$$\mu\left(N,T\right)=\frac{1}{2m}\left(\frac{\pi j\hbar}{L}\right)^2+\mu_j\left(N_j,T\right),\ \epsilon_j\left(\mathbf{q}\right)=\frac{1}{2m}\left(\left(\frac{\pi j\hbar}{L}\right)^2+q^2\right) \quad (25)$$

where μ_j is the chemical potential of a $2D$ system of N_j fermions in the band j. If we are dealing with a dilute gas, then μ_j depends only on the number of particles $z_j=2N_jL^2/\pi$ in this band,

$$z_j=\vartheta_T\ln\left(1+\exp\left(\frac{\mu_j}{T}\right)\right)=\vartheta_T\ln\left(1+\exp\left(\frac{\mu}{T}-\frac{j^2}{\vartheta_T}\right)\right),$$

and

$$\mu_j=T\ \ln\left(\exp\left(\frac{z_j}{\vartheta_T}\right)-1\right) \quad (26)$$

where

$$\vartheta_T=\frac{2mTL^2}{\pi^2\hbar^2}$$

describes the ratio of the temperature to the energy of zero-point oscillations in the well of the width L. This equation should be used to express the chemical potential via the total number of particles $z=2NL^2/\pi$,

$$z=\vartheta_T\sum_{j=1}^{\infty}\ln\left[\exp\left(\frac{\mu}{T}-\frac{j^2}{\vartheta_T}\right)+1\right] \quad (27)$$

The solution of this equation $\mu\left(z\right)$ at $T=0$ is given by Eq. (15).

We will give the transport coefficients for high-temperature systems of particles with the Boltzmann distribution function when

$$z=\vartheta_T\exp\left(\frac{\mu}{T}\right)\Theta,\ \mu=T\ \ln\left(\frac{z}{\vartheta_T\Theta}\right),\ \Theta\left(\vartheta_T\right)\equiv\sum_{j=1}^{\infty}\exp\left(-\frac{j^2}{\vartheta_T}\right).$$

The transport equation (5) in dimensionless variables $\chi_j(q)$,

$$n_j(\mathbf{q}) = n_j^{(0)}(q)\left(1 - \frac{FL^3}{\pi^4 T\ell^2}\chi_j(q)\cos\theta\right)$$

assumes the form

$$u^{1/2} = \frac{1}{2\pi^2 L^2\ell^2}\{\chi_j(q)\left[\begin{array}{c}\frac{1}{4}u^2(\eta_1(u,u_{jj}) - \eta_0(u,u_{jj})) \\ +uj^2(\gamma_1(u,u_{jj}) - \gamma_0(u,u_{jj})) + j^4(\zeta_1(u,u_{jj}) - \zeta_0(u,u_{jj}))\end{array}\right] + \sum_{j'\neq j}^{S(u,j)} j^2 j'^2[\chi_{j'}\zeta_1(u,u_{jj'}) - \chi_j\zeta_0(u,u_{jj'})]\} \quad (28)$$

while the mobility (conductivity) is

$$\sigma_{yy} = \sigma_{zz} = \sum_{j=1}^{\infty}\sigma_{yy}^{(j)} = -\frac{e^2L^2}{2\pi^4\hbar\ell^2}\frac{z}{\vartheta_T^2\Theta}\sum_{j=1}^{\infty}\exp\left(-\frac{j^2}{\vartheta_T}\right)\int u^{1/2}\chi_j(q)\exp\left[-\frac{u}{\vartheta_T}\right]du \quad (29)$$

Here

$$u = q^2\left(\frac{L}{\pi\hbar}\right)^2,\ S(u,j) = \mathrm{Int}\left[\left(u+j^2\right)^{1/2}\right],\ u_{jj'} = u + j^2 - j'^2 = q'^2\left(\frac{L}{\pi\hbar}\right)^2,$$

and $\zeta_{0,1}(u,u_{jj})$, $\eta_{0,1}(u,u_{jj})$, and $\gamma_{0,1}(u,u_{jj})$ are the zeroth and first angular Fourier harmonics of the functions

$$\begin{aligned}\zeta(\mathbf{q}-\mathbf{q}') &= \zeta\left(q^2+q'^2-2qq'\cos\varphi\right) = \zeta(u,u_{jj},\cos\varphi), \quad (30)\\ \eta(\mathbf{q}-\mathbf{q}') &= \zeta(\mathbf{q}-\mathbf{q}')[1-\cos\varphi]^2,\ \gamma(\mathbf{q}-\mathbf{q}') = \zeta(\mathbf{q}-\mathbf{q}')[1-\cos\varphi]\end{aligned}$$

over the angle φ between the vectors $\mathbf{q}$ and $\mathbf{q}'$. In essence, the variable $u = (qL/\pi\hbar)^2$ plays the same role as the Fermi momenta $z_j = \left(q_F^{(j)}L/\pi\hbar\right)^2$ for degenerate systems in the previous Section.

In the Gaussian case (7), integration in (28) leads to the same set of equations (16) with the only difference that z_i should be substituted by u. The situation is again non-analytic since the summation in (30) for off-diagonal transitions over j' should be performed up to the value $S(u,j)$ which is not only different for each j, *i.e.,* for each equation, but also depends on momentum q and exhibits step-like jumps at certain values of $u = q^2(L/\pi\hbar)^2$. However, this non-analyticity manifests itself more noticeably in the integrands (29) rather than in the transport coefficients themselves which are fairly smooth. Finally, the conductivity (mobility) is equal to

$$\begin{aligned}\sigma_{yy} &= \sum_{j=1}^{\infty}\sigma_{yy}^{(j)} = \frac{e^2NL^4}{\pi^5\hbar\ell^2}\Pi\left(\vartheta_T,\frac{R}{L}\right), \quad (31)\\ \Pi(x,y) &= \frac{1}{x^2\Theta(x)\,y^2}\sum_{j=1}^{\infty}\int\chi_j(u)\exp\left(-\frac{j^2+u^2}{x}\right)du\end{aligned}$$

Function $\Pi(x,y)$ is plotted in Figure 4 for $y = R/L = 0.05$ and in Figure 5 for $y = R/L = 0.5;\ 1$.

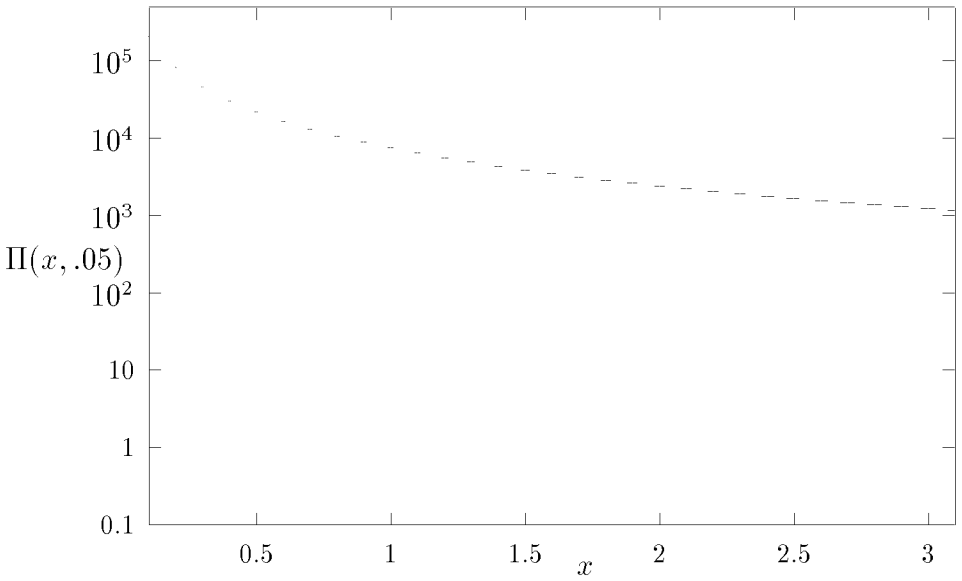

Figure 4. Function $\Pi(x, y)$, Eq.(31), for $y = R/L = 0.05$

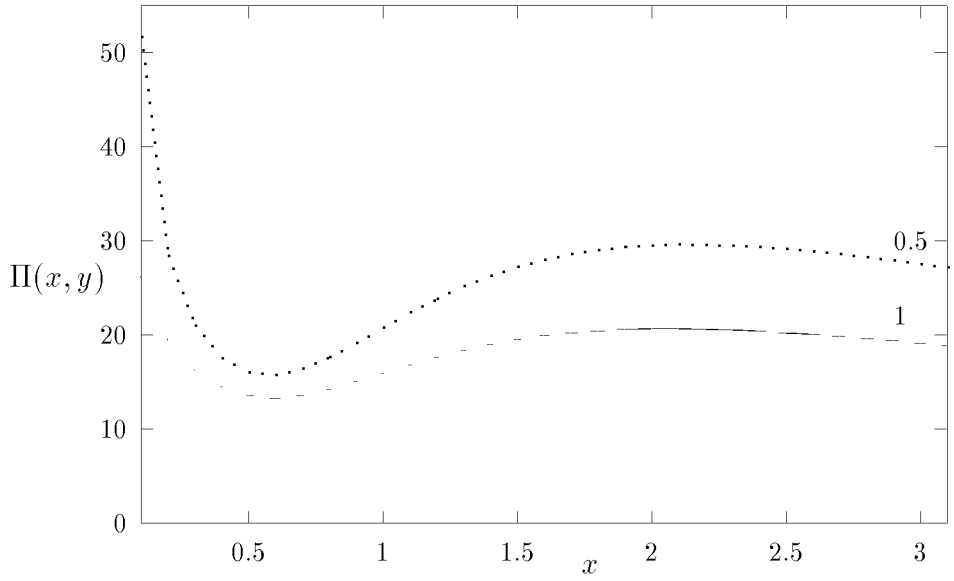

Figure 5. Function $\Pi(x, y)$, Eq.(31), for $y = R/L = 0.5$ (solid line) and 1 (dotted line)

In the Boltzmann temperature range, the diffusion coefficient can be expressed via mobility as

$$D_{yy,zz} = -\frac{\pi\hbar^2}{e^2 m}\sigma_{yy} / \sum_j \int \frac{\partial n_j}{\partial \epsilon}\, d\epsilon = \frac{T\sigma_{yy}}{e^2 N} = \frac{TL^4}{\pi^5 \hbar \ell^2} \Pi\left(\vartheta_T, \frac{R}{L}\right), \tag{32}$$

while the mean free path

$$\mathcal{L} = \sigma < q > / e^2 N = \frac{(mT)^{1/2} L^4}{\pi^5 \hbar \ell^2} \Pi\left(\vartheta_T, \frac{R}{L}\right) \tag{33}$$

The difference between the functions $\Pi(x)$ in Figures 4,5 by several orders of magnitude is not surprising. Since $x = \vartheta_T \sim (L/\lambda)^2$ (λ is the particle wavelength), Figure 4 is plotted in the region $L \sim \lambda$. On the other hand, $y = R/L = 0.05$ is rather small meaning that $R/\lambda \ll 1$. As it was explained in [10] (and is confirmed by the present calculation), condition $R/\lambda \ll 1$ corresponds to a nearly specular quantum reflection, and, therefore, to large particle mean free paths. Thus the large values of $\Pi(x)$ in Figure 4. In Figure 5, $y = R/L \sim R/\lambda \sim 1$. This case corresponds to the most effective scattering of particles by surface inhomogeneities and to the smallest values of the mean free path.

5. Summary and discussion

In summary, we calculated mobility and diffusion coefficients for ballistic particles in ultra-thin films with random rough boundaries when the motion of particles across the film is quantized. We obtained simple and explicit expressions for transport coefficients via the correlation function of surface inhomogeneities, particle density N and the film thickness L. The particle transport along the film is a non-trivial function of two dimensionless parameters, NL^2 and R/L, where R is the correlation radius of surface inhomogeneities. The most important consequence of a discrete character of the particle spectrum for the motion across the film is the non-analytic low-temperature dependence of the transport coefficients on the film thickness and the density of particles with the singularities at the critical values of NL^2.

The strength these singularities strongly depends on the correlation radius of surface inhomogeneities R. In the case of short-range correlations of surface inhomogeneities, the low-temperature dependence of transport coefficients on particle density and film thickness has a pronounced saw-like structure. The saw teeth become smaller and the saw-like structure gradually disappears with increasing correlation radius. Finally, for long-range correlations one gets not very well pronounced kinks, instead of the saw teeth, at the critical values of density and/or thickness at which the number of occupied levels changes by one.

Though both the amplitude an the correlation radius of surface inhomogeneities affect the particle scattering by the walls, the dependence of transport coefficients on

the amplitude of the surface inhomogeneities ℓ, in contrast to their dependence on the correlation radius R, is quite trivial, and reduces to a multiplicative factor $1/\ell^2$.

In general, the non-analytic nature of the curves is explained by the singularities in the (low-temperature) distribution of fermions over a system of discrete energy subbands. However, the sharp discontinuities on the saw-like curves for transport coefficients are caused not by the singularities in the density of state, but mostly by the interband transitions caused by the scattering from wall inhomogeneities.

The occupation of a new, higher energy subband leads to two transport effects: to the direct transport contribution of the particles from this new band, and to the opening of new scattering channels for particles in all already occupied bands (interband transitions to and from the new band). The first effect is proportional to the number of particles in the new band and is small. For this reason the singularity of the transport coefficients reduces, in the absence of interband transitions, to a series of kinks corresponding to the occupancy of the higher bands. On the other hand, the opening of new scattering channels with the interband transitions to and from newly occupied bands affects particles from *all* already occupied bands thus increasing dramatically the total effective scattering cross-section in a step-like manner. If one artificially freezes these transitions, the transport curves will exhibit kinks rather than the saw teeth.

Not surprisingly, the contribution of interband transitions depends exponentially on the ratio of the particle wavelength to the correlation radius of the surface inhomogeneities, and decreases rapidly with increasing correlation radius of surface roughness (*i.e.,* with flattening of surface inhomogeneities). The emerging picture is more complicated than that described in[17, 29, 15] because, in contrast to bulk impurities, surface inhomogeneities can have a relatively large correlation length.

The parameterization of transport parameters in this paper is slightly different from [10]. In the case of the mean free path it is, probably, better to use, instead of (20) , (33), the parameterization in the form [10]

$$\mathcal{L} \sim \frac{L^2 R}{\ell^2} f\left(R/\lambda\right)$$

with the minimum at $R \sim \lambda$. The transformation of the results to this form is fairly straightforward in both degenerate and Boltzmann regions. As usual, the information on the mean free path allows one to calculate quantum interference corrections and to determine the localization length.

6. Acknowledgments

This work was supported by NSF grant DMR-9412769.

7. References

[1] Beckmann P, and Spizzichino A. 1963 *The Scattering of Electromagnetic Waves from Random Surfaces* (Pergamon, N.Y.)

[2] Bass F G and Fuks I M 1979 *Wave Scattering from Statistically Rough Surfaces* (Pergamon, N.Y.)

[3] DeSanto J A, and Brown D S 1986 *Analytical Techniques for Multiple Scattering from Rough Surfaces*, Prog.Optics, v. XXIII, ed. E.Wolf (North-Holland, Amsterdam)

[4] Willis J R 1988 *Mathematical Aspects of Scattering from Rough Cracks*, in: Mathematic Modeling in Non-Destructive Testing, eds. M.Blakemore, G.A.Georgiou (Clarendon, Oxford) p.57

[5] *Interactions of Atoms and Molecules with Solid Surfaces*, eds. V.Bortolani, N.H.March, and M.P.Tosi (Plenum, NY) 1990

[6] Ogilvy J A 1992 *Theory of Wave Scattering from Random Surfaces* (Adam Hilger, Bristol)

[7] Voronovich A G 1994 *Wave Scattering at Rough Surface* (Springer, Berlin)

[8] Okulov V I and Ustinov V V 1979 Sov.J. Low Temp.Phys. **5** 101

[9] Ando T, Fowler A B, and Stern F 1982 Rev.Mod.Phys. **54 437**

[10] Meyerovich A E and Stepaniants S 1995 Phys.Rev. B **51** 17116

[11] Meyerovich A E and Stepaniants S 1994 Phys.Rev.Lett. **73** 316

[12] Fishman G and Calecki D 1989 Phys.Rev.Lett. **62** 1302

[13] Reiss G, Hastreiter E, Brückl H, and Vancea J 1991 Phys.Rev. B**43** 5176

[14] Nicolic K and MacKinnon A 1994 Phys.Rev.Lett. **50** 11008

[15] Makarov N M, Moroz A V, and Yampol'skii V A 1995 Phys.Rev. B **52** 6087

[16] Tesanovic Z, Jaric M V, and Maekawa S 1986 Phys.Rev.Lett. **57** 2760

[17] Trivedi N and Ashcroft N W 1988 Phys.Rev. B **38** 12298

[18] Konrady J A Jr. 1974 J.Acoust.Soc.Am., **56** 1687

[19] Bass F, Freulicher V D, and Fuks I 1974 IEEE Trans. AP-**22** 278; 288

[20] Abrabanel H D I 1980 J.Acoust.Soc.Am. **68** 1459

[21] McGurn A and Maradudin A 1984 Phys.Rev. B **30** 3136

[22] Arseyev P 1987 JETP Lett. **45** 163 [1987 Pis'ma Zh.Eksp.&Teor.Fiz. **45** 132]

[23] Thorsos E I and Jackson D R 1989 J.Acoust.Soc.Am. **86** 261

[24] Goldstein R E, Pesci A I, and Romero-Rochin V 1990 Phys.Rev. A **41** 5504

[25] Isers A B, Puzenko A A, and Fuks I M 1991 J.Electromag.Waves and Appl. **5** 1419

[26] Kozub V I and Krokhin A A 1993 J.Phys.: Condens. Matter **5** 9135

[27] Glazman L I, Lesovik G B, Khmel'nitskii D E, and Shekhter R I 1988 JETP Lett. **48** 238 [1988 Pis'ma Zh.Eksp.&Teor.Fiz. **48** 218]; Wharam D A *et al* 1988 J.Phys.C **21** L209; van Wees B J *et al* 1988 Phys.Rev.Lett. **60** 848

[28] Beskok A, Karniadakis, G E, and Trimmer W, 1996 J.Fluids Eng. **118** in print

[29] Sandomirskii V B 1968 Sov.Phys.-JETP **25** 101 [1968 Zh.Eksp.&Teor.Fiz. **52** 158]

8. Appendix. Classical and Semi-Classical Motion Across the Channels

In the classical limit, when the distance between the bands with different j becomes negligible, the above results should coincide with the results of classical calculations in [10]. The transition to the classical limit corresponds to thick films or to the states with large quantum numbers, $j \gg 1$, when the interlevel transitions are accompanied by relatively small changes of the quantum number, $1 \sim \delta j \ll j$. The coordinate transformation (1) and the effective Hamiltonian (3) are, obviously, the same in the classical and quantum cases. The matrix elements of the effective bulk distortion (3) are

$$V_{\mathbf{q}j,\mathbf{q}'j'} = \frac{\xi\left(\mathbf{q}-\mathbf{q}'\right)}{mL}\left[\begin{array}{c}\delta_{jj'}\left(\frac{\pi^2 j^2}{L^2}+\frac{1}{4}\left(q^2-q'^2\right)\right)+ \\ \frac{1}{2}\left((-1)^{j+j'}+1\right)\frac{\left(1-\delta_{jj'}\right)jj'}{j^2-j'^2}\left(q^2-q'^2\right)\end{array}\right] \tag{34}$$

In the quasiclassical (continuous) limit we should substitute $j\hbar/L$ and $j'\hbar/L$ by p_x and p'_x and assume that $j, j' \gg 1$. Then the matrix elements (34) coincide exactly with the classical matrix elements in [10] with the $\delta_{jj'}$-terms giving rise to $\delta\left(p_x-p'_x\right)$, and the terms with $\left(1-\delta_{jj'}\right)/\left(j-j'\right)$- to $\delta'\left(p_x-p'_x\right)$.

The collision integral (4) contains the squares of the matrix elements $V_{\mathbf{q}j,\mathbf{q}'j'}$. The calculation of $\left\langle\left|V_{\mathbf{q}j,\mathbf{q}'j'}\right|^2\right\rangle$ for the quantum matrix elements (34) is trivial since $\delta_{jj'}^2=\delta_{jj'}$, $\left(1-\delta_{jj'}\right)^2 = 1-\delta_{jj'}$, and $\delta_{jj'}\left(1-\delta_{jj'}\right) = 0$. However, a calculation of the squares of the classical matrix elements in the continuous limit, as in Ref.[10], involves the use of not very well defined squares of the δ-functions $\delta\left(p_x-p'_x\right)$ and $\delta'\left(p_x-p'_x\right)$. In our calculation [10] we used the following approximation for such a product of the δ-functions:

$$\delta'\left(p_x-p'_x\right)\delta\left(p_x-p'_x\right) = -\frac{1}{2}\left[\delta^2\left(p_x-p'_x\right)\right]' \simeq -\frac{L}{2\hbar}\delta'\left(p_x-p'_x\right) \tag{35}$$

An unambiguous calculation procedure requires the transition to the classical expressions only after the quantum calculation of $\left\langle\left|V_{\mathbf{q}j,\mathbf{q}'j'}\right|^2\right\rangle$ when the problem with the squares of the δ-functions does not arise (an alternative is the use of the bell-shaped functions instead of δ-functions, *e.g.,* in the presence of dissipation; this option is more complicated). The use of the quantum expression for $\left\langle\left|V_{\mathbf{q}j,\mathbf{q}'j'}\right|^2\right\rangle$ on the basis of Eq.(34) with the consequent transition to the quasiclassical limit shows that the exact expression for the above product of the δ-functions (35) has the form

$$\delta'\left(p_x-p'_x\right)\delta\left(p_x-p'_x\right) = -\delta'\left(\mathbf{p}_x-\mathbf{p}'_x\right)/2p_x$$

This leads to a more accurate classical analog of the transition probability,

$$W\left(\mathbf{p},\mathbf{p}'\right) = \frac{2\pi}{\hbar}\left\langle\left|V_{\mathbf{j}\mathbf{q},j'\mathbf{q}'}\right|^2\right\rangle = \frac{\zeta\left(\mathbf{q}-\mathbf{q}'\right)}{4\pi L^2 m^2}\delta\left(\epsilon-\epsilon'\right)\times \tag{36}$$

$$\left[2p_x^4\delta\left(p_x-p_x'\right)+\frac{\Omega^2}{4}\delta''\left(p_x-p_x'\right)\right],$$

$$\Omega\left(\mathbf{p},\mathbf{p}'\right) = \left(\mathbf{q}-\mathbf{q}'\right)\cdot\left(p_x\mathbf{q}+p_x'\mathbf{q}'\right),$$

than Eq.(18) of [10].

The corresponding change in the classical collision integral does not result in any significant changes in the expressions for the classical transport coefficients. The *only* improvement should be the substitution of the functions

$$\frac{d\,\sin\theta}{\alpha+4\tan^4\theta}$$

in the integrands for all transport coefficients in Ref. [10] by

$$\frac{d\,\sin\theta}{\alpha+4\beta\tan^4\theta+8\tan^4\theta}$$

where

$$\alpha\left(u\right) = (5/2)\ {}_1F_1\left(7/2,4,-u^2\right)/\,{}_1F_1\left(3/2,2,-u^2\right),$$
$$\beta\left(u\right) = (3/2)\ {}_1F_1\left(5/2,3,-u^2\right)/\,{}_1F_1\left(3/2,2,-u^2\right)$$

This change in the analytical expressions leads to more accurate results. However, the numerical change is not very significant. This small numerical change is illustrated in Figures 6,7 for the functions $f_B\left(x\right)$ and $f_F\left(x\right)$ which describe the transport coefficients and the mean free path [10] for Boltzmann and Fermi gases,

$$\sigma = \frac{32}{\pi^{3/2}}\frac{e^2L^2R^2N}{\hbar\ell^2}xf_B\left(x\right),\ x=\frac{\hbar}{\left(4mT\right)^{1/2}R},$$
$$f_B\left(x\right) = x^4\int\frac{\exp\left[-x^2z^2/\cos^2\theta\right]}{{}_1F_1\left(3/2,2,-z^2\right)}\frac{dz}{\cos^2\theta}\frac{d\theta}{\alpha+4\beta\tan^4\theta+8\tan^4\theta} \qquad (37)$$

and

$$\sigma = \frac{\sqrt{2}}{\pi^3}\frac{e^2L^2}{\hbar\ell^2R}x^2f_F\left(x\right),\ x=\sqrt{2}p_FR/\hbar,$$
$$f_B\left(x\right) = \frac{1}{x^3}\int\frac{1}{{}_1F_1\left(3/2,2,-x^2\cos^2\theta\right)}\frac{1}{\cos^2\theta}\frac{d\sin\theta}{\alpha+4\beta\tan^4\theta+8\tan^4\theta} \qquad (38)$$

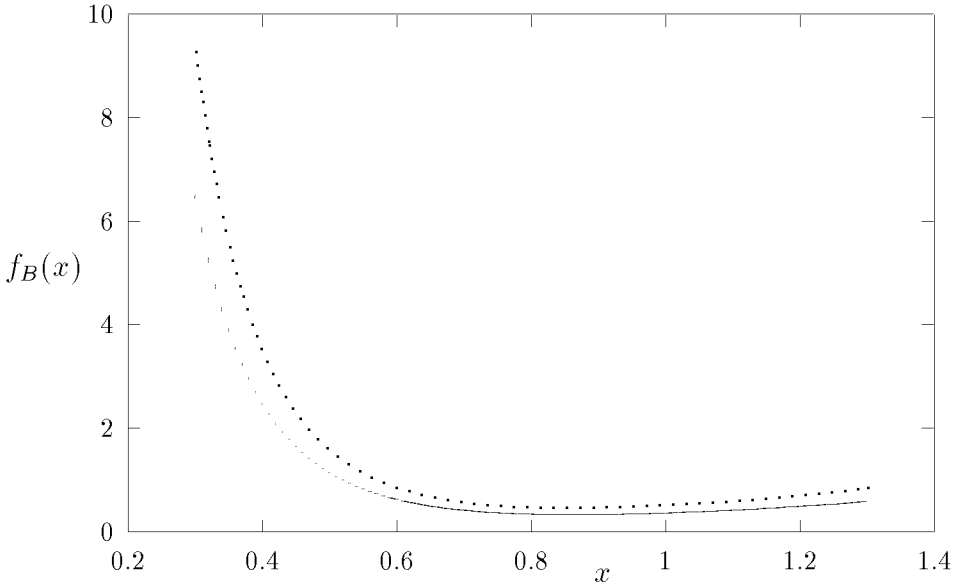

Figure 6. Function $f_B(x)$; solid line - Eq.(37), dotted line - result of Ref.[10].

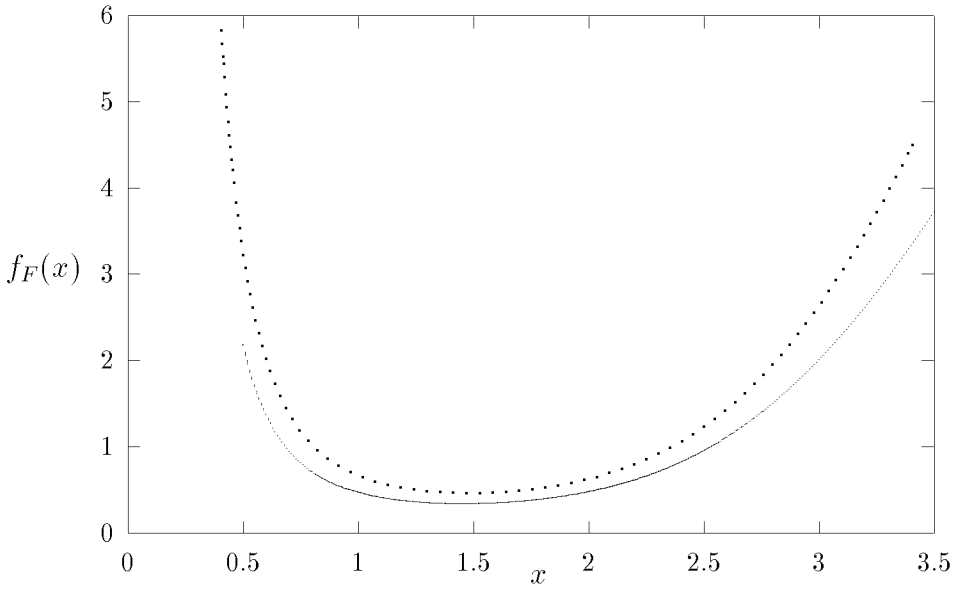

Figure 7. Function $f_F(x)$; solid line - Eq.(38), dotted line - result of Ref.[10].

9. FIGURE CAPTIONS

Figure 1. $\Phi(z, R/L)$, Eq.(18), as a function of density $z = 2NL^2/\pi$ for the correlation radius $R/L = 0.05$. Solid line - exact calculation; dotted line - calculation without

interband transitions (without off-diagonal terms in the collision integral (6))

Figure 2. $\Phi(z, R/L)$, Eq.(18), as a function of density $z = 2NL^2/\pi$ for the correlation radius $R/L = 1; 3; 5$. The curves are labled by the values of R/L.

Figure 3. $\Phi(z, R/L)$, Eq.(18), as a function of density $z = 2NL^2/\pi$ for $R/L = 1; 5$ calculated without interlevel transitions (without off-diagonal terms in the collision integral (6)). The curves are labled by the values of R/L.

Figure 4. Function $\Pi(x, y)$, Eq.(31), for $y = R/L = 0.05$

Figure 5. Function $\Pi(x, y)$, Eq.(31), for $y = R/L = 0.5$ (solid line) and 1 (dotted line)

Figure 6. Function $f_B(x)$; solid line - Eq.(37), dotted line - result of Ref.[10]

Figure 7. Function $f_F(x)$; solid line - Eq.(38), dotted line - result of Ref.[10]